

A Universal Layer-by-Layer Solution-Processing Approach for Efficient Non-fullerene Organic Solar Cells

Rui Sun^{1#}, Jing Guo^{1#}, Chenkai Sun², Tao Wang¹, Zhenghui Luo³, Zhuohan Zhang⁴, Xuechen Jiao^{5*}, Weihua Tang^{4*}, Chuluo Yang^{3,6*}, Yongfang Li^{2*}, Jie Min^{1*}

¹The Institute for Advanced Studies, Wuhan University, Wuhan 430072, China
E-mail: min.jie@whu.edu.cn

²CAS Research/Education Center for Excellence in Molecular Sciences, CAS Key Laboratory of Organic Solids, Institute of Chemistry, Chinese Academy of Sciences, Beijing 100190, China.

E-mail: liyf@iccas.ac.cn

³Hubei Key Lab on Organic and Polymeric Optoelectronic Materials, Department of Chemistry, Wuhan University, Wuhan 430072, China

E-mail: clyang@whu.edu.cn

⁴Key Laboratory of Soft Chemistry and Functional Materials, Ministry of Education, Nanjing University of Science and Technology, Nanjing 210094, China

E-mail: whtang@njust.edu.cn

⁵Department of Materials Science and Engineering, Monash University, Victoria, Australia; Australian Synchrotron, Clayton, VIC, Australia

E-mail: xuechen.jiao@monash.edu

⁶College of Materials Science and Engineering, Shenzhen University, Shenzhen, 518060, China.

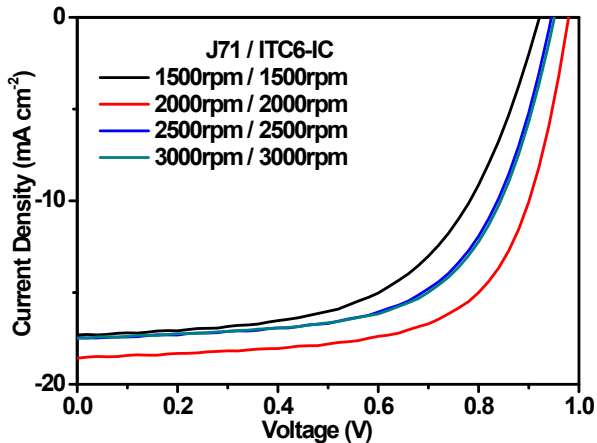


Figure S1. J - V curves of devices based on J71/ITC6-IC LbL films with different D/A coating speeds under the illumination of an AM 1.5G solar simulator, 100 mW cm⁻².

Table S1. Photovoltaic parameters of devices based on J71/ITC6-IC LbL films with different D/A coating speeds under the illumination of an AM 1.5G solar simulator, 100 mW cm⁻².

Thickness [nm] (Speed, rpm)	V_{oc} [V]	J_{sc} [mA cm ⁻²]	FF [%]	PCE(PCE ^a) [%]
73nm/60nm (1500/1500 rpm)	0.921	17.30	57.85	9.22(9.08)
64nm/42nm (2000/2000 rpm)	0.979	18.57	66.41	12.08(11.51)
56nm/36nm (2500/2500 rpm)	0.948	18.12	63.41	10.90(10.57)
43nm/34nm (3000/3000 rpm)	0.951	17.49	63.11	10.50(10.23)

^aThe values in square bracket are the average PCE obtained from six devices.

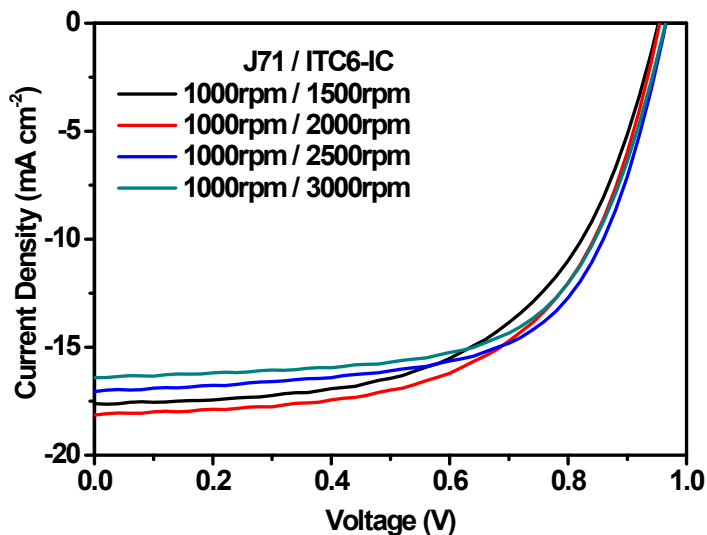


Figure S2. $J-V$ curves of devices based on J71/ITC6-IC LbL films with different coating speeds of acceptor materials under the illumination of an AM 1.5G solar simulator, 100 mW cm^{-2} .

Table S2. Photovoltaic parameters of devices based on J71/ITC6-IC LbL films with different coating speeds of acceptor materials under the illumination of an AM 1.5G solar simulator, 100 mW cm^{-2} .

Speed(rpm)	Voc [V]	Jsc [mA cm $^{-2}$]	FF [%]	PCE(PCE ^a) [%]
(Donor/Acceptor)				
1000/1500	0.953	17.61	57.87	9.71(9.28)
1000/2000	0.954	18.13	59.47	10.29(10.01)
1000/2500	0.965	17.05	63.81	10.50(10.23)
1000/3000	0.964	16.41	63.92	10.11(9.57)

^aThe values in square bracket are the average PCE obtained from six devices.

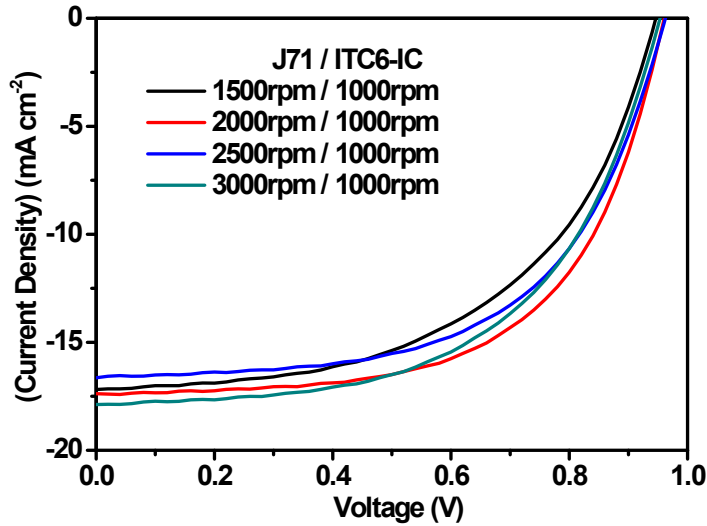


Figure S3. $J-V$ curves of devices based on J71/ITC6-IC LbL films with different coating speeds of donor materials under the illumination of an AM 1.5G solar simulator, 100 mW cm^{-2} .

Table S3. Photovoltaic parameters of devices based on J71/ITC6-IC LbL films with different coating speeds of donor materials under the illumination of an AM 1.5G solar simulator, 100 mW cm^{-2} .

Speed(rpm)	Voc [V]	Jsc [mA cm $^{-2}$]	FF [%]	PCE(PCE ^a) [%]
(Donor/Acceptor)				
1500/1000	0.970	16.11	52.22	8.16(8.08)
2000/1000	0.960	17.38	60.16	10.04(9.98)
2500/1000	0.962	16.64	58.04	9.29(9.02)
3000/1000	0.953	17.88	56.41	9.59(9.25)

^aThe values in square bracket are the average PCE obtained from six devices.

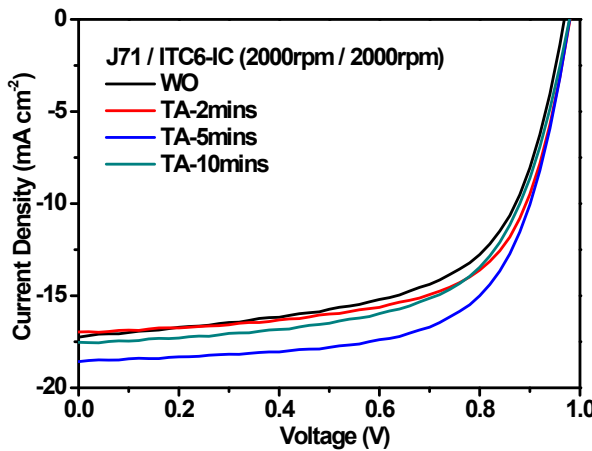


Figure S4. *J-V* curves of devices based on J71/ITC6-IC LbL films spin-coated by 2000 rpm for both donor and acceptor layers with different annealing time at 150 °C under the illumination of an AM 1.5G solar simulator, 100 mW cm⁻².

Table S4. Photovoltaic parameters of devices based on J71/ITC6-IC LbL films spin-coated by 2000 rpm for both donor and acceptor layers with different annealing time at 150 °C under the illumination of an AM 1.5G solar simulator, 100 mW cm⁻².

TA treatment at 150 °C	Voc [V]	Jsc [mA cm ⁻²]	FF [%]	PCE(PCE ^a) [%]
wo	0.968	17.24	61.70	10.29(9.87)
2 min	0.962	16.96	63.50	10.36 (9.93)
5 min	0.979	18.57	66.41	12.08 (11.51)
10 min	0.980	17.52	65.56	11.25 (10.84)

^aThe values in square bracket are the average PCE obtained from six devices .

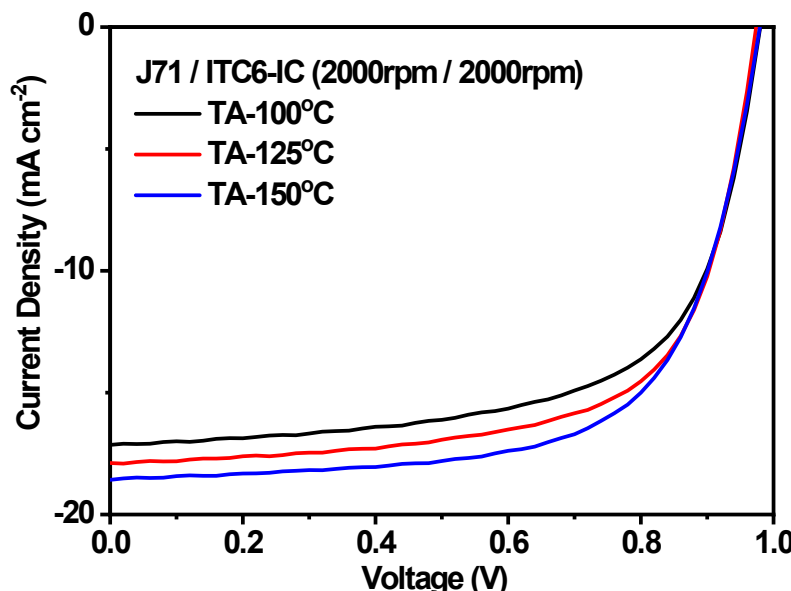


Figure S5. $J-V$ curves of devices based on J71/ITC6-IC LbL films spin-coated by 2000 rpm for both donor and acceptor layers with different annealing temperatures under the illumination of an AM 1.5G solar simulator, 100 mW cm^{-2} .

Table S5. Photovoltaic parameters of devices based on J71/ITC6-IC LbL films spin-coated by 2000 rpm for both donor and acceptor layers with different annealing temperatures under the illumination of an AM 1.5G solar simulator, 100 mW cm^{-2} .

TA temperature (5 mins)	Voc [V]	Jsc [mA cm $^{-2}$]	FF [%]	PCE(PCE ^a) [%]
100 °C	0.982	17.14	64.03	10.77 (10.31)
120 °C	0.973	17.88	66.80	11.62 (11.12)
150 °C	0.979	18.57	66.41	12.08(11.51)

^aThe values in square bracket are the average PCE obtained from six devices.

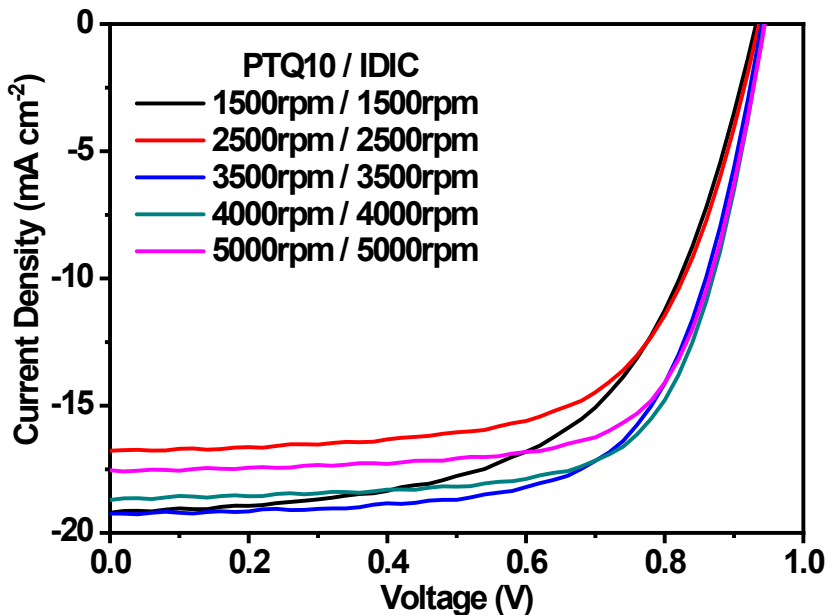


Figure S6. $J-V$ curves of devices based on PTQ10/IDIC LbL films with different D/A coating speeds under the illumination of an AM 1.5G solar simulator, 100 mW cm^{-2} .

Table S6. Photovoltaic parameters of devices based on PTQ10/IDIC LbL films with different D/A coating speeds under the illumination of an AM 1.5G solar simulator, 100 mW cm^{-2} .

Thickness [nm] (Speed, rpm)	Voc [V]	Jsc [mA cm $^{-2}$]	FF [%]	PCE(PCE ^a) [%]
90/79 (1500/1500 rpm)	0.931	19.20	58.99	10.55(10.02)
82/72	0.936	16.76	64.55	10.13(9.70)

(2500/2500 rpm)				
73/54	0.940	19.23	67.04	12.12(12.01)
(3500/3500 rpm)				
62/44	0.943	18.70	69.66	12.29(12.03)
(4000/4000 rpm)				
51/38	0.944	17.53	70.26	11.63(11.43)
(5000/5000 rpm)				

^aThe values in square bracket are the average PCE obtained from six devices.

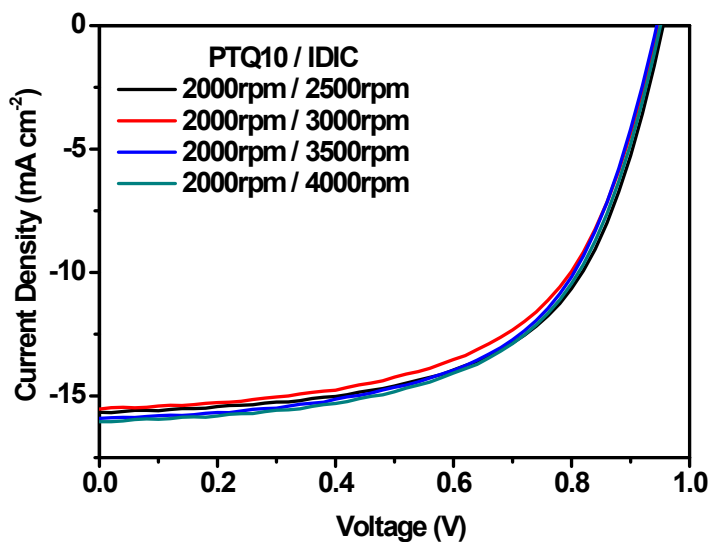


Figure S7. *J-V* curves of devices based on PTQ10/IDIC LbL films with different coating speeds of acceptor materials under the illumination of an AM 1.5G solar simulator, 100 mW cm⁻².

Table S7. Photovoltaic parameters of devices based on PTQ10/IDIC LbL films with different coating speeds of acceptor materials under the illumination of an AM 1.5G solar simulator, 100 mW cm⁻².

Speed(rpm)	Voc	Jsc	FF	PCE(PCE ^a)
(Donor/Acceptor)	[V]	[mA cm ⁻²]	[%]	[%]
2000/2500	0.955	15.66	60.36	9.03(8.88)
2000/3000	0.946	15.53	58.69	8.62(8.42)
2000/3500	0.944	15.91	59.28	8.90(8.73)
2000/4000	0.950	16.04	59.14	9.02(8.31)

^aThe values in square bracket are the average PCE obtained from six devices.

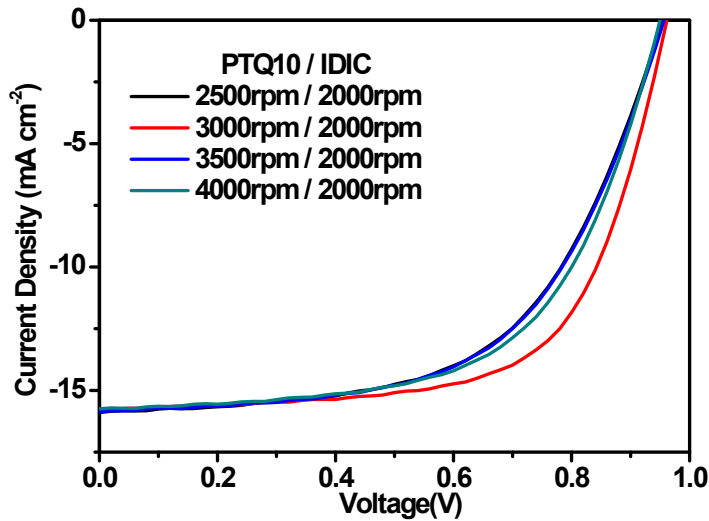


Figure S8. J - V curves of devices based on PTQ10/IDIC LbL films with different coating speeds of donor materials under the illumination of an AM 1.5G solar simulator, 100 mW cm^{-2} .

Table S8. Photovoltaic parameters of devices based on PTQ10/IDIC LbL films with different coating speeds of donor materials under the illumination of an AM 1.5G solar simulator, 100 mW cm^{-2} .

Speed(rpm)	Voc [V]	Jsc [mA cm⁻²]	FF	PCE(PCE ^a)
(Donor/Acceptor)				[%]
2500/2000	0.954	15.89	57.66	8.74(8.32)
3000/2000	0.961	15.78	65.09	9.87(9.46)
3500/2000	0.956	15.85	57.92	8.77(8.41)
4000/2000	0.949	15.74	60.20	8.99(8.54)

^aThe values in square bracket are the average PCE obtained from six devices.

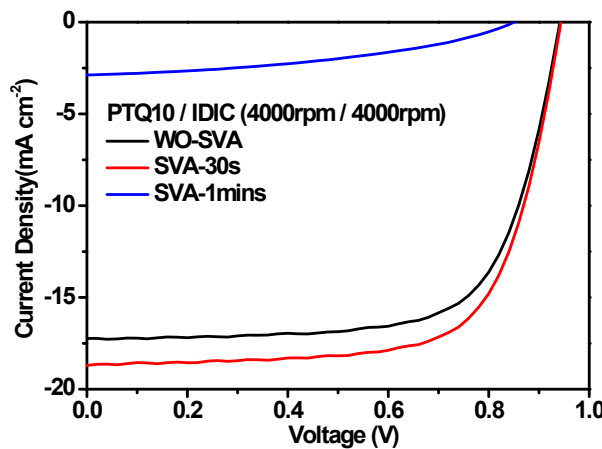


Figure S9. J - V curves of devices based on PTQ10 / IDIC LbL films spin-coated by 4000 rpm for both donor and acceptor layers with different solvent vapor annealing time after TA treatment 5 mins at 140°C under the illumination of an AM 1.5G solar simulator, 100 mW cm^{-2} .

Table S9. Photovoltaic parameters of devices based on PTQ10/IDIC LbL films spin-coated by 4000 rpm for both donor and acceptor layers with different solvent vapor annealing time after TA treatment 5 mins at 140 °C under the illumination of an AM 1.5G solar simulator, 100 mW cm⁻².

SVA time after TA 140 °C	Voc [V]	Jsc [mA cm ⁻²]	FF [%]	PCE(PCE ^a) [%]
w0	0.941	17.23	69.87	11.33 (11.22)
30s	0.943	18.70	69.66	12.29 (12.03)
60s	0.850	2.87	40.90	1.00 (0.869)

^aThe values in square bracket are the average PCE obtained from six devices.

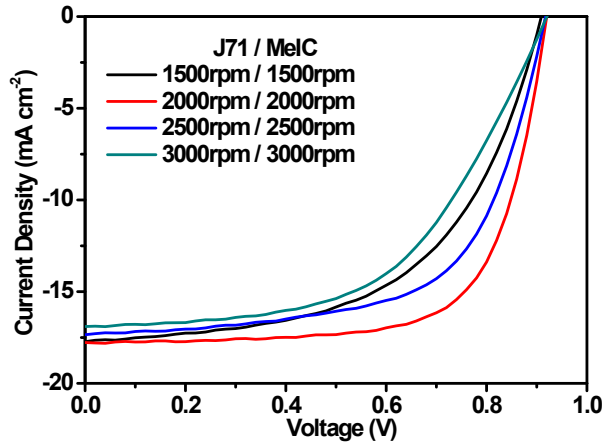


Figure S10. *J-V* curves of devices based on J71/MeIC LbL films with different D/A coating speeds under the illumination of an AM 1.5G solar simulator, 100 mW cm⁻².

Table S10. Photovoltaic parameters of devices based on J71/MeIC LbL films with different D/A coating speeds under the illumination of an AM 1.5G solar simulator, 100 mW cm⁻².

Thickness [nm] (Speed, rpm)	Voc [V]	Jsc [mA cm ⁻²]	FF [%]	PCE(PCE ^a) [%]
74/45 (1500/1500 rpm)	0.909	17.72	55.46	8.93(6.01)
64/36 (2000/2000 rpm)	0.919	17.77	69.89	11.43(11.19)
56/26 (2500/2500 rpm)	0.923	17.35	62.94	10.07(9.98)
44/20 (3000/3000 rpm)	0.920	16.90	54.30	8.44(8.32)

^aThe values in square bracket are the average PCE obtained from six devices.

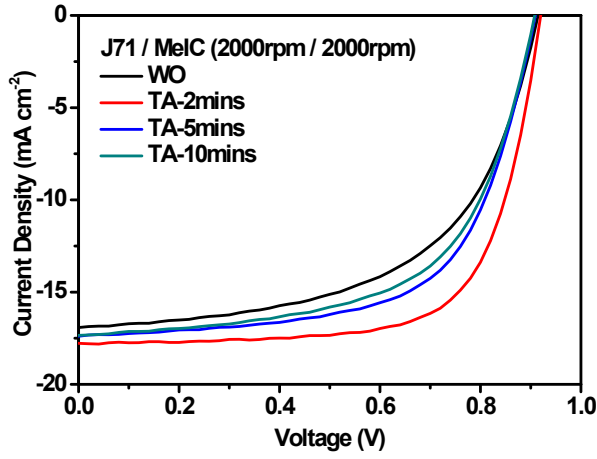


Figure S11. *J-V* curves of devices based on J71/MeIC LbL films spin-coated by 2000 rpm for both donor and acceptor layers with different annealing time at 150 °C under the illumination of an AM 1.5G solar simulator, 100 mW cm⁻².

Table S11. Photovoltaic parameters of devices based on J71/MeIC LbL films spin-coated by 2000 rpm for both donor and acceptor layers with different annealing time at 150 °C under the illumination of an AM 1.5G solar simulator, 100 mW cm⁻².

TA treatment at 150 °C	Voc [V]	Jsc [mA cm ⁻²]	FF [%]	PCE(PCE ^a) [%]
wo	0.914	16.92	56.69	8.76 (8.65)
2 min	0.919	17.77	69.89	11.43(11.19)
5 min	0.909	17.39	63.07	9.96 (9.75)
10 min	0.907	17.34	60.39	9.49 (9.25)

^aThe values in square bracket are the average PCE obtained from six devices.

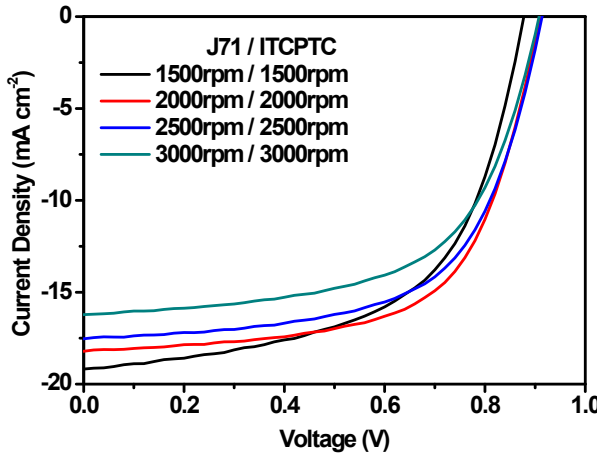


Figure S12. *J-V* curves of devices based on J71/ITCPTC LbL films with different D/A coating speeds under the illumination of an AM 1.5G solar simulator, 100 mW cm⁻².

Table S12. Photovoltaic parameters of devices based on J71/ITCPTC LbL films with different D/A coating speeds under the illumination of an AM 1.5G solar simulator, 100 mW cm⁻².

Thickness [nm] (Speed, rpm)	Voc [V]	Jsc [mA cm ⁻²]	FF [%]	PCE(PCE ^a) [%]
74/40 (1500/1500 rpm)	0.885	19.17	57.96	9.83(9.40)
64/30 (2000/2000 rpm)	0.909	18.21	63.07	10.44 (10.06)
56/26 (2500/2500 rpm)	0.913	17.53	61.86	9.90(8.77)
44/22 (3000/3000 rpm)	0.907	16.21	60.39	8.87(8.57)

^aThe values in square bracket are the average PCE obtained from six devices.

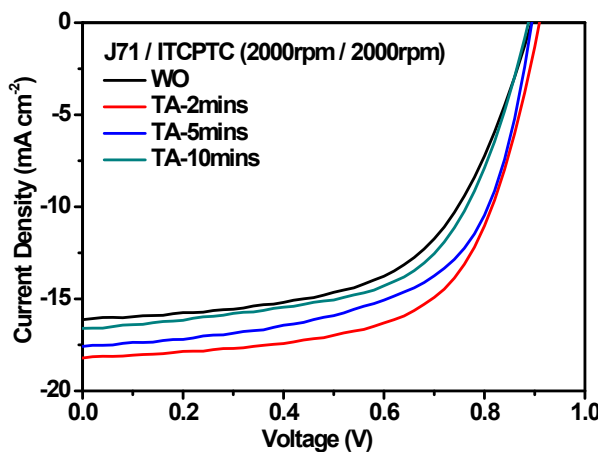


Figure S13. *J-V* curves of devices based on J71/ITCPTC LbL films spin-coated by 2000 rpm for both donor and acceptor layers with different annealing time at 150 °C under the illumination of an AM 1.5G solar simulator, 100 mW cm⁻².

Table S13. Photovoltaic parameters of devices based on J71/ITCPTC LbL films spin-coated by 2000 rpm for both donor and acceptor layers with different annealing time at 150 °C under the illumination of an AM 1.5G solar simulator, 100 mW cm⁻².

TA treatment at 150 °C	Voc [V]	Jsc [mA cm ⁻²]	FF [%]	PCE(PCE ^a) [%]
wo	0.893	16.12	58.40	8.41 (8.13)
2 min	0.909	18.21	63.07	10.44 (10.06)
5 min	0.894	17.57	61.20	9.62 (8.98)
10 min	0.887	16.60	60.32	8.88 (8.38)

^aThe values in square bracket are the average PCE obtained from six devices.

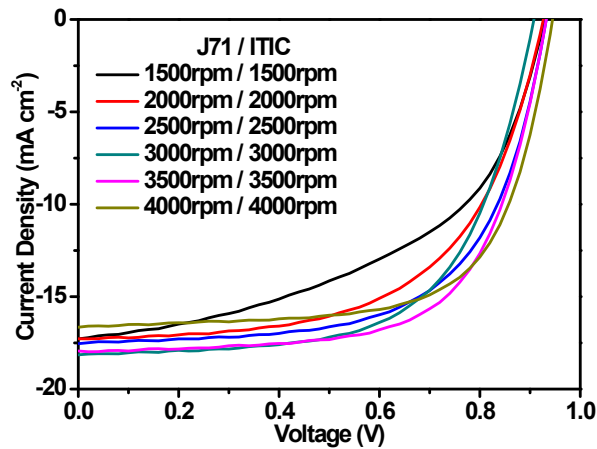


Figure S14. *J-V* curves of devices based on J71/ITIC LbL films with different D/A coating speeds under the illumination of an AM 1.5G solar simulator, 100 mW cm⁻².

Table S14. Photovoltaic parameters of devices based on J71/ITIC LbL films with different D/A coating speeds under the illumination of an AM 1.5G solar simulator, 100 mW cm⁻².

Thickness [nm] (Speed, rpm)	Voc [V]	Jsc [mA cm ⁻²]	FF [%]	PCE(PCE ^a) [%]
91/53 (1500/1500 rpm)	0.928	17.21	49.97	7.98 (7.75)
79/48 (2000/2000 rpm)	0.926	17.28	58.15	9.30(9.06)
71/42 (2500/2500 rpm)	0.932	17.48	62.50	10.18(9.76)
67/36 (3000/3000 rpm)	0.907	18.10	62.01	10.17(9.84)
55/29 (3500/3500 rpm)	0.932	17.98	65.33	10.94(10.47)
49/23 (4000/4000 rpm)	0.944	16.59	67.30	10.53(10.30)

^aThe values in square bracket are the average PCE obtained from six devices.

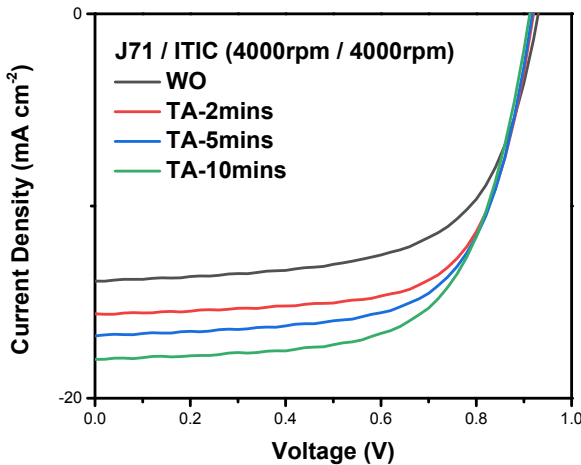


Figure S15. J - V curves of devices based on J71/ITIC LbL films spin-coated by 2000 rpm for both donor and acceptor layers with different annealing time at 150 °C under the illumination of an AM 1.5G solar simulator, 100 mW cm⁻².

Table S15. Photovoltaic parameters of devices based on J71/ITIC LbL films spin-coated by 2000 rpm for both donor and acceptor layers with different annealing time at 150 °C under the illumination of an AM 1.5G solar simulator, 100 mW cm⁻².

TA treatment at 150 °C	Voc [V]	Jsc [mA cm ⁻²]	FF [%]	PCE(PCE ^a) [%]
wo	0.930	13.90	63.37	8.19(7.89)
2 min	0.920	15.60	68.09	9.77 (9.51)
5 min	0.917	16.75	66.17	10.17 (10.03)
10 min	0.932	17.98	65.33	10.94(10.47)

^aThe values in square bracket are the average PCE obtained from six devices.

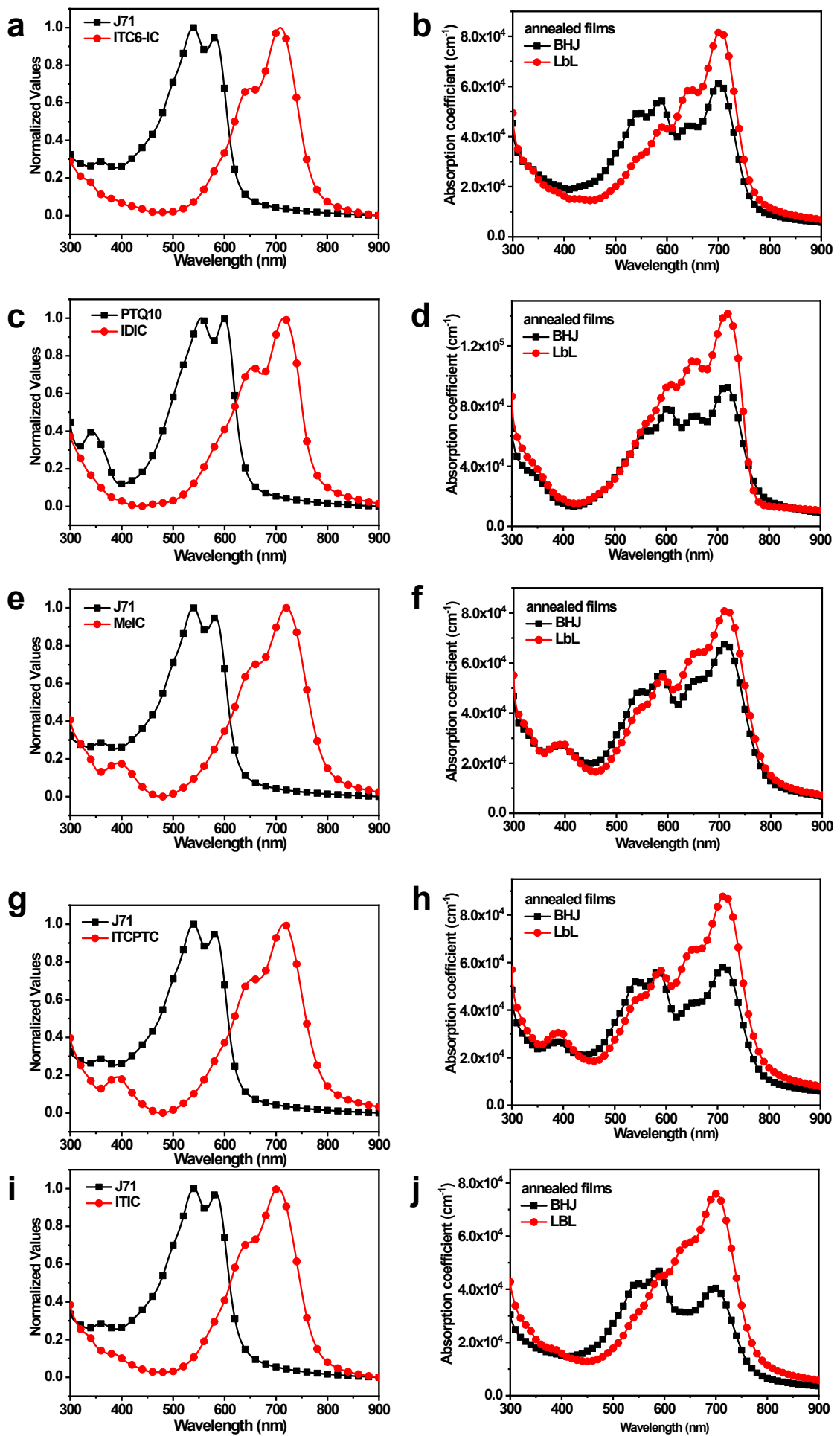


Figure S16. UV-Vis absorption spectra of pristine J71 and ITC6-IC films (a) and J71:ITC6-IC BHJ and J71/ITC6-IC LbL films treated by thermal annealing (TA) (b); pristine PTQ10 and IDIC films (c) and PTQ10:IDIC BHJ and PTQ10/IDIC LbL films treated by TA (d); pristine J71 and MeIC films (e) and J71:MeIC BHJ and J71/MeIC LbL films treated by TA (f); pristine J71 and ITCPTC films (g) and J71:ITCPTC BHJ and J71/ITCPTC LbL films treated by TA (h); pristine J71 and ITIC films (i) and J71:ITIC BHJ and J71/ITIC LbL films treated by TA (j).

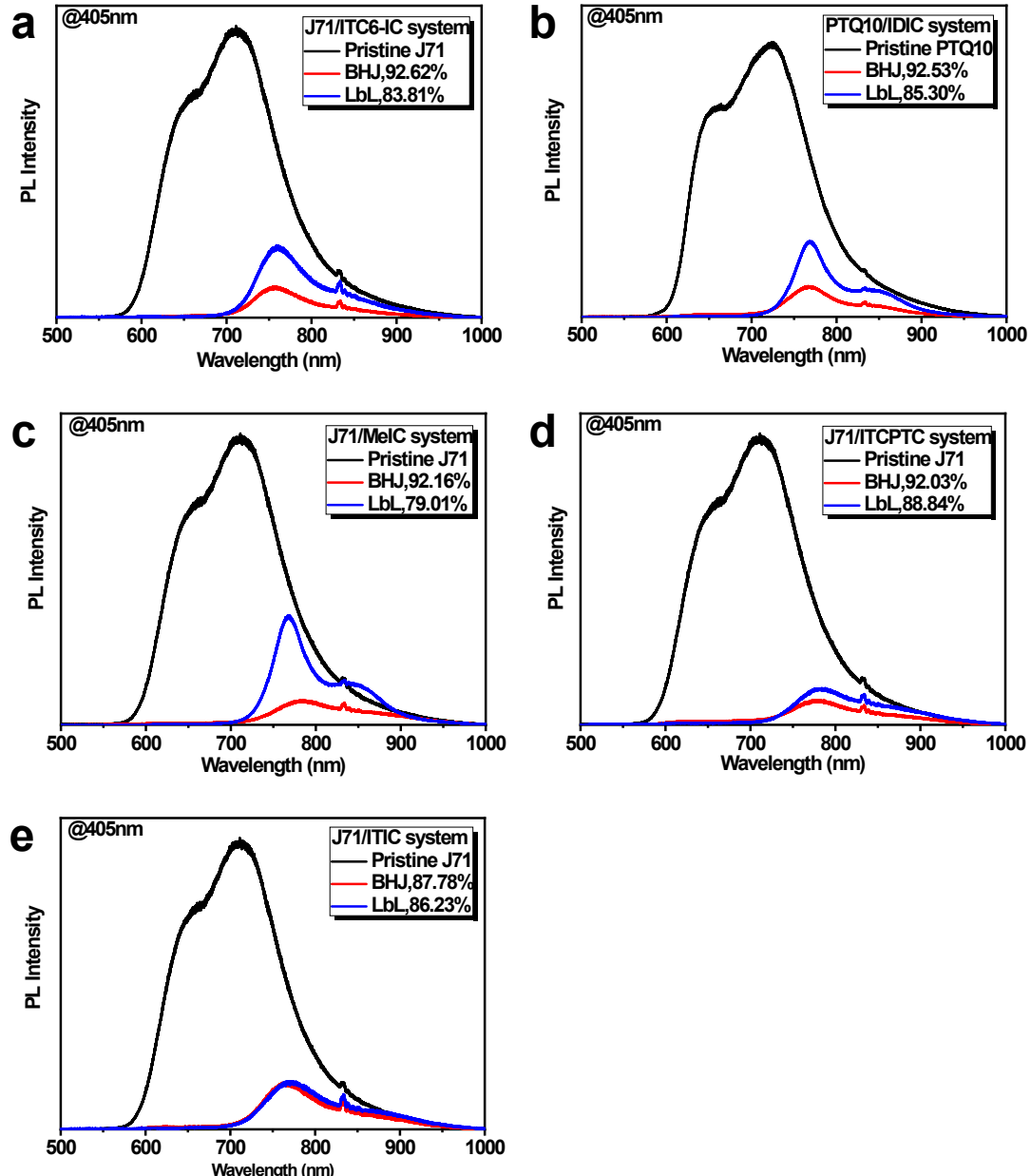


Figure S17. PL measurements of pristine J71 and PTQ10 films as well as the relevant systems including (a) J71:ITC6-IC BHJ and J71/ITC6-IC LbL films, (b) PTQ10:IDIC BHJ and PTQ10/IDIC LbL films, (c) J71:MeIC BHJ and J71/MeIC LbL films, (d) J71:ITCPTC BHJ and J71/ITCPTC LbL films and (e) J71:ITIC BHJ and J71/ITIC LbL films.

Table S16. Combination sheet for BHJ and LbL layers in the screening. (1) The onset wavelength of the optical absorption of various blend layers. (2) The optical bandgap (E_g) in eV estimated from the absorption spectrum of blends. (3) values of the V_{oc} are measured under one sun illumination. (4) Values of the E_{loss} ($E_g - qV_{oc}$). (5) The differences of E_{loss} between BHJ systems and LbL systems.

Active layers	BHJ or LbL	λ_{onset}^a [nm]	E_g^b [eV]	V_{oc}^c [V]	E_{loss}^d [eV]	ΔE_{loss}^e [e mV]
J71&ITC6-IC	BHJ	782	1.585	0.938	0.647	61
	LbL	790	1.565	0.979	0.586	
PTQ10&IDIC	BHJ	795	1.559	0.939	0.621	22
	LbL	804	1.542	0.943	0.599	
J71&MeIC	BHJ	795	1.559	0.908	0.652	31
	LbL	805	1.540	0.919	0.621	
J71&ITCPTC	BHJ	788	1.573	0.881	0.693	34
	LbL	791	1.567	0.909	0.658	
J71&ITIC	BHJ	780	1.590	0.930	0.660	38
	LbL	798	1.554	0.932	0.622	

^aCast from chloroform solution. ^bBandgap estimated from the onset wavelength (λ_{onset}) of the optical absorption: $E_g^{opt} = 1240/\lambda_{onset}$. ^c V_{oc} are measured under one sun illumination. ^dCalculated energy gap losses in devices via a formula ($E_{loss} = E_g - qV_{oc}$). ^eThe differences of energy gap losses between BHJ and LbL systems via a formula ($\Delta E_g = E_{loss_BHJ} - E_{loss_LbL}$).

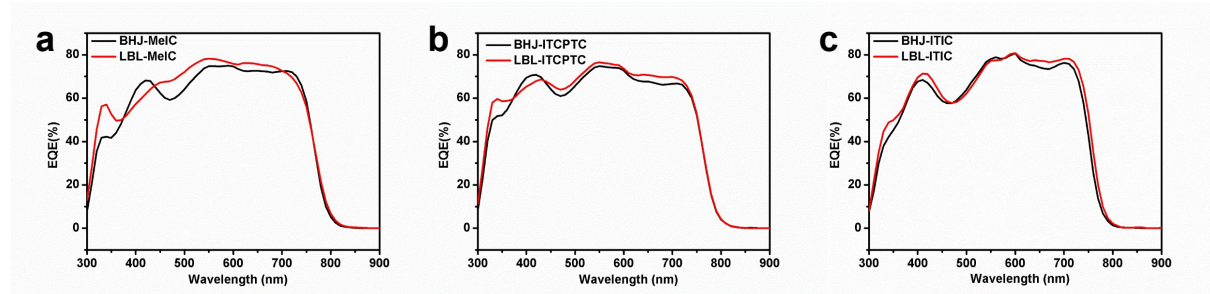


Figure S18. EQE spectra of BHJ and LbL solar cells based J71 with MeIC, ITCPTC and ITIC acceptors, respectively.

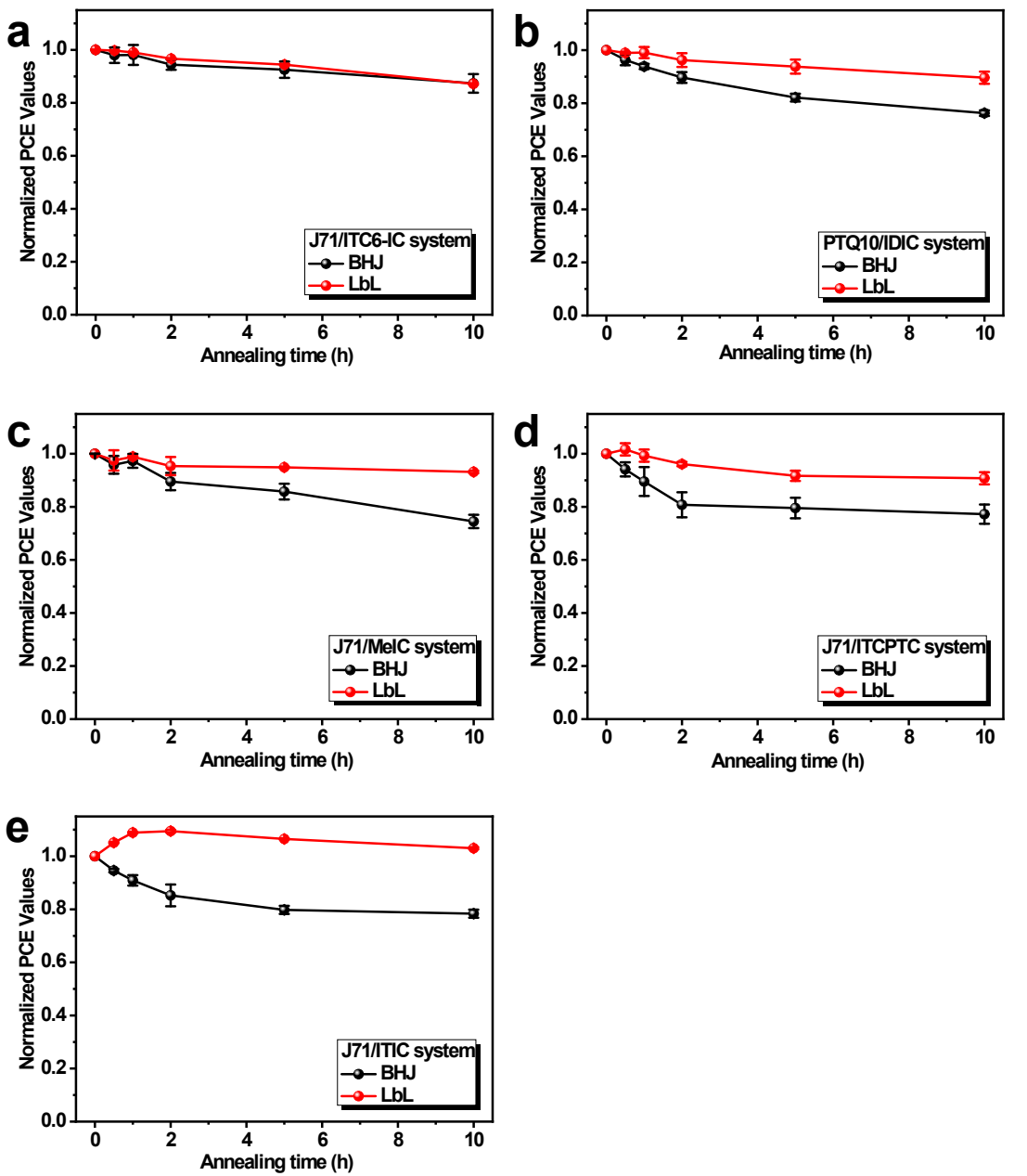


Figure S19. Variation of normalized PCE of the devices based on BHJ and LbL structures, annealed at 100 °C. These devices include (a) J71/ITC6-IC system, (b) PTQ10/IDIC system (c) J71/MeIC system, (d) J71/ITCPTC system and (e) J71/ITIC system.

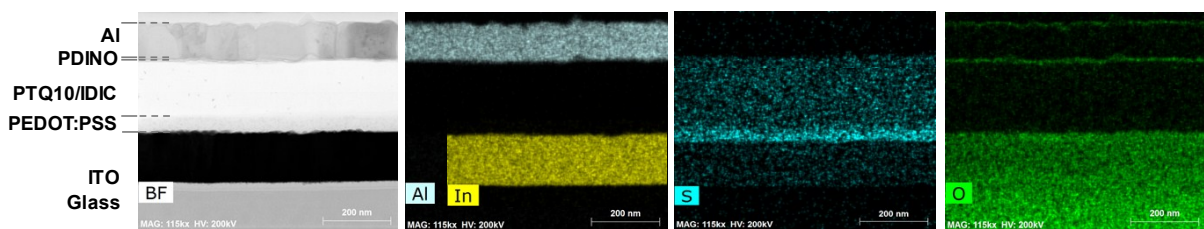


Figure S20. TEM image of the cross-section and EDS elemental (O, S, Al, In) maps. The scale bar is 200 nm.

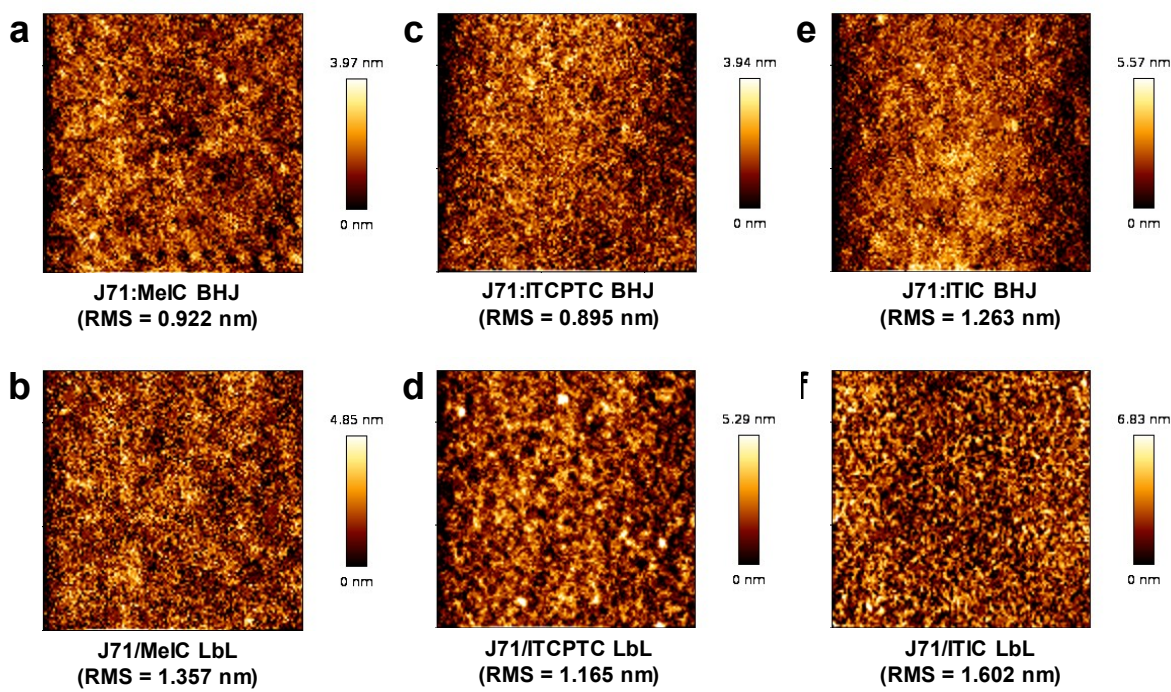


Figure S21. Contact mode AFM surface scans (size: $5 \times 5 \mu\text{m}^2$) of films of: (a) J71:MeIC BHJ (RMS = 0.922 nm), (b) J71/MeIC LbL (RMS = 1.357 nm), (c) J71:ITCPTC BHJ (RMS = 0.895 nm), (d) J71/ITCPTC LbL (RMS = 1.165 nm), (e) J71:ITIC BHJ (RMS = 1.263 nm), and (f) J71/ITIC LbL (RMS = 1.602 nm).

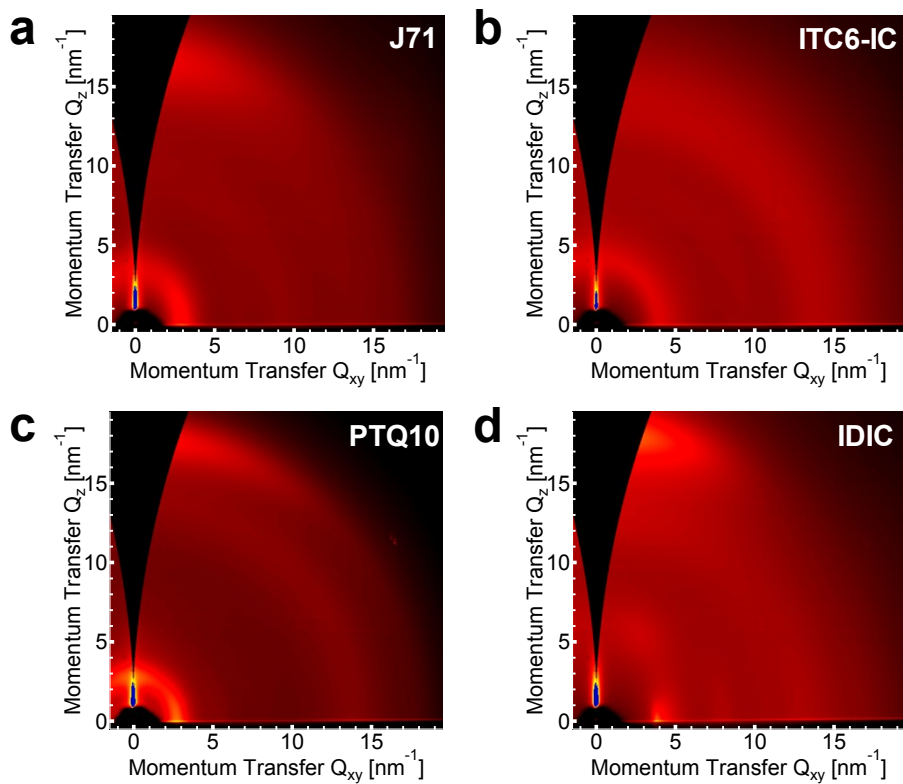


Figure S22. 2D GIWAXS patterns of (a) pristine J71 film, (b) pristine ITC6-IC film, (c) pristine PTQ10 film, (d) pristine IDIC film. All of the films were acquired at the critical incident angle of 0.13° .

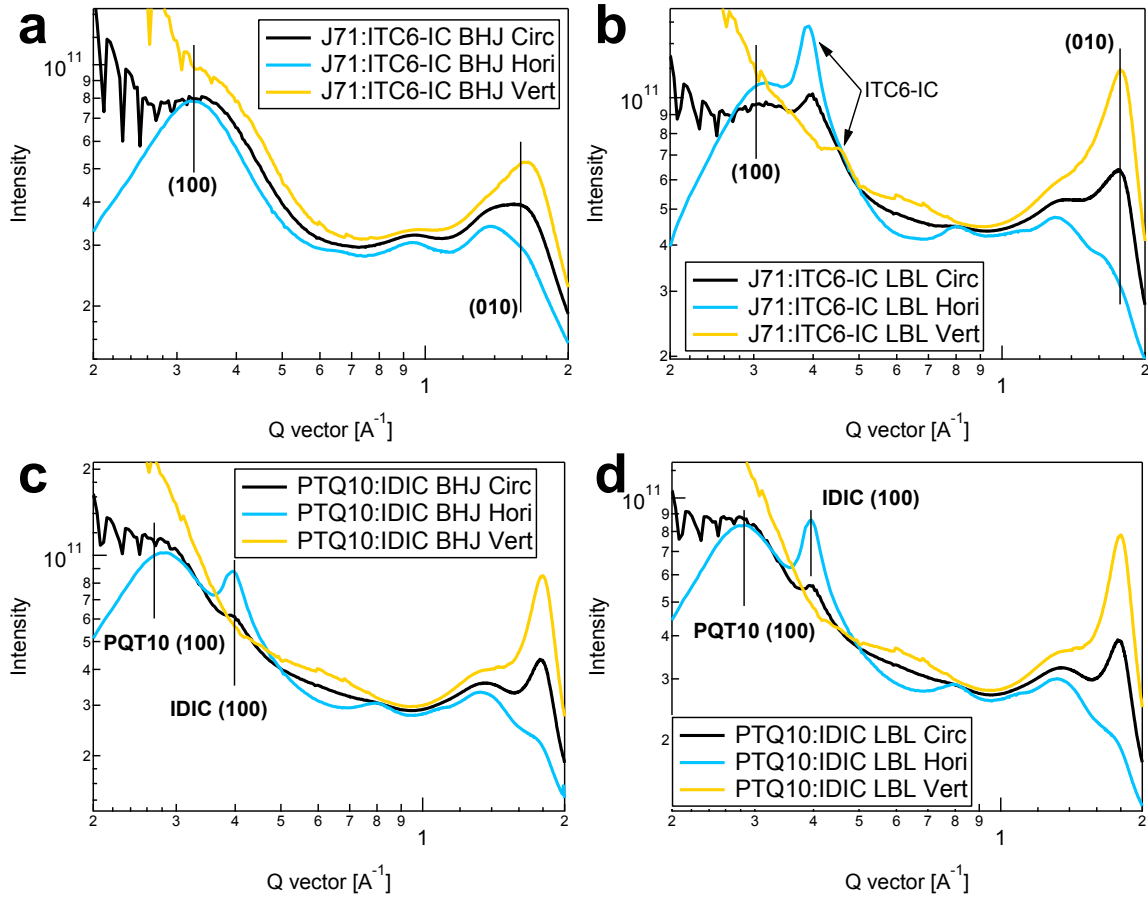


Figure S23. 1D GIWAXS profiles of (a) J71:ITC6-IC BHJ film, (b) J71/ITC6-IC LbL film, (c) PTQ10:IDIC BHJ film and (d) PTQ10/IDIC LbL film. All films were acquired at the critical angle of 0.13° .

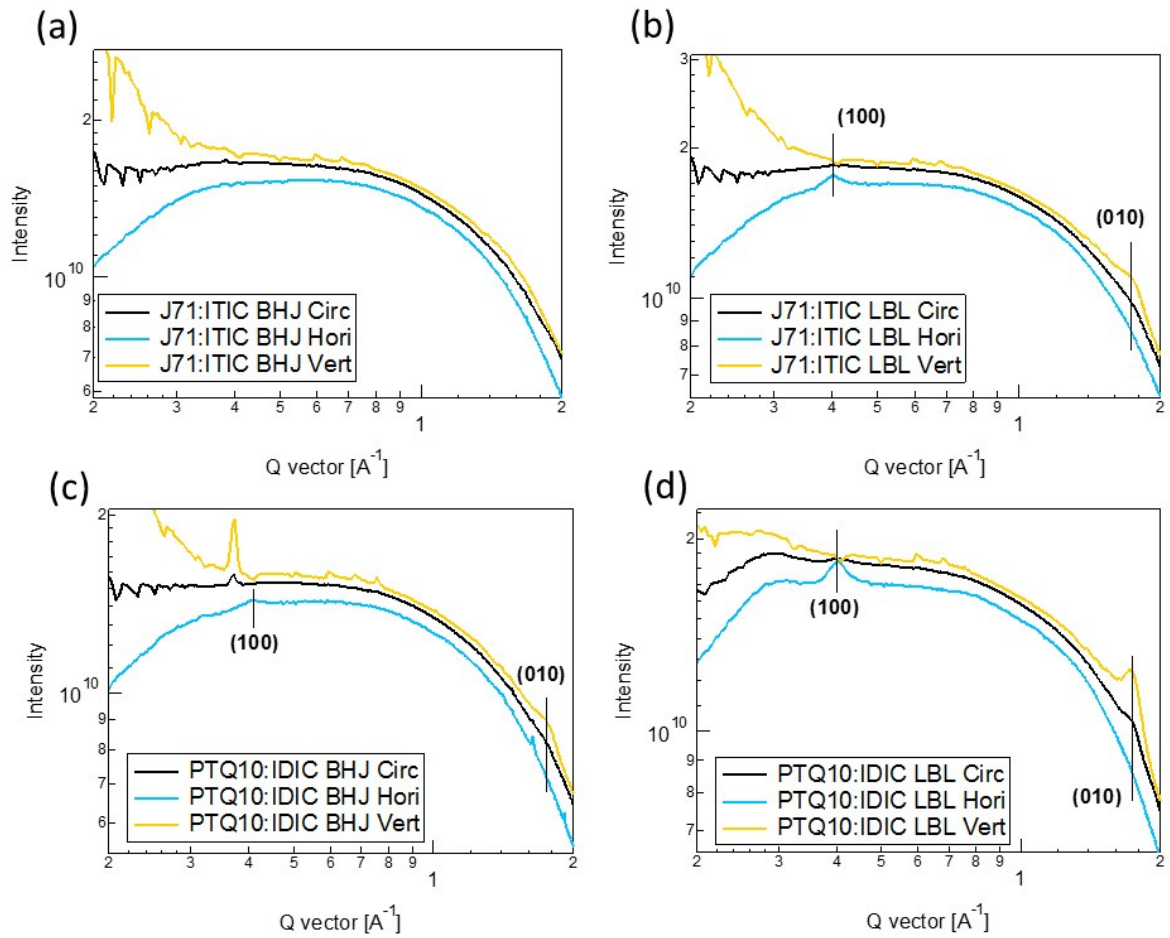


Figure S24. 1D GIWAXS profiles of (a) J71:ITC6-IC BHJ film, (b) J71/ITC6-IC LbL film, (c) PTQ10:IDIC BHJ film and (d) PTQ10/IDIC LbL film. All films were acquired at the shallow incident angle of 0.02°. Note the spike appeared along the vertical direction in PTQ10:IDIC BHJ blend was an artifact from the parasitic scattering.

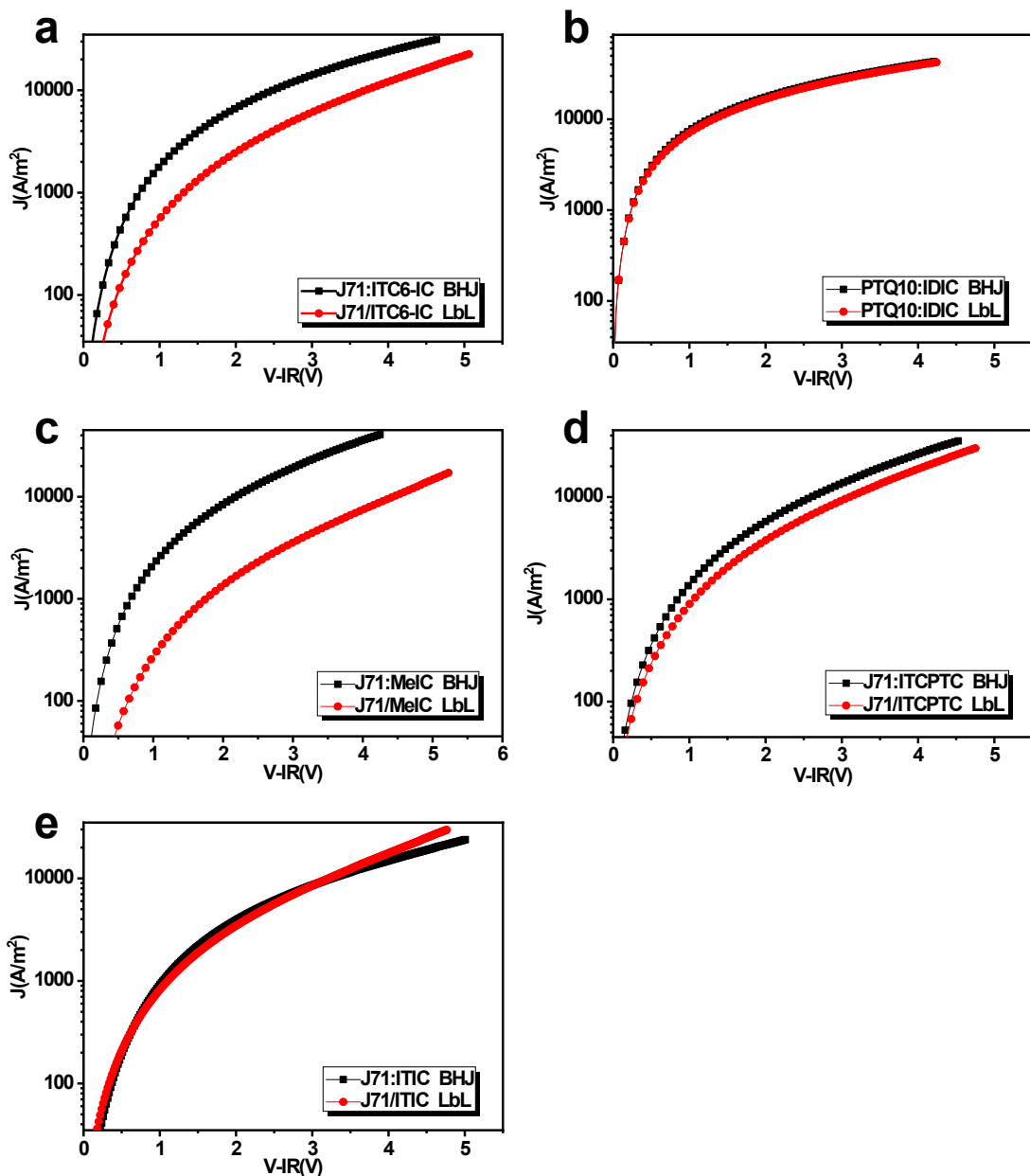


Figure S25. The dark J - V characteristics of (a) J71:ITC6-IC, (b) PTQ10:IDIC, (c) J71:MeIC, (d) J71:ITCPTC and (e) J71:ITIC based hole-only devices with respect to the BHJ and LbL structures. The solid lines represent the best fitting using the SCLC model.

Table S17. Summary of the fitting data for hole-only devices based on the three molecules based on Mott-Gurney law.

Semiconductor layers	Layer type	Thickness (nm)	Ave. Mobility ^a ($\text{cm}^2\text{V}^{-1}\text{s}^{-1}$)
J71:ITC6-IC	BHJ	92	5.20×10^{-4}
	LbL	105	2.02×10^{-4}
PTQ10:IDIC	BHJ	112	7.23×10^{-3}

	LbL	105	7.10×10^{-3}
J71:MeIC	BHJ	103	5.56×10^{-4}
	LbL	100	3.95×10^{-4}
J71:ITCPTC	BHJ	90	2.22×10^{-4}
	LbL	93	1.36×10^{-4}
J71:ITIC	BHJ	102	2.09×10^{-4}
	LbL	86	1.04×10^{-4}

^aan average value based on six devices with the same thickness.

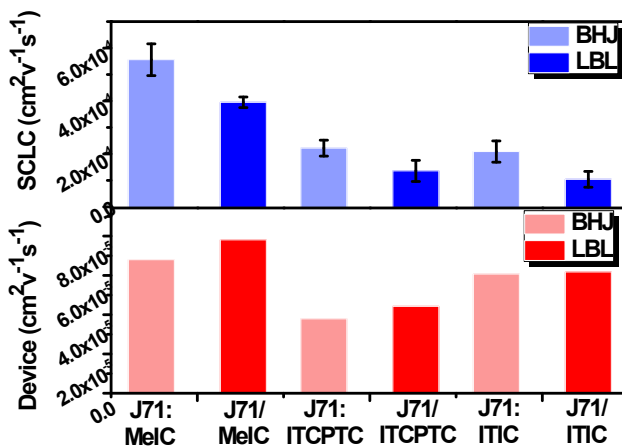


Figure S26. Hole only mobilities measured in single carrier diodes obtained from J71:MeIC, J71:ITCPTC, and J71:ITIC films. For the SCLC measurements, the values were obtained based on six devices of each type, and the error bars represent plus or minus 1 standard deviation from the mean values (SCLC mobility). Carrier mobilities of the these three different NFA systems calculated from time delayed collection field photo-CELIV (device mobility).

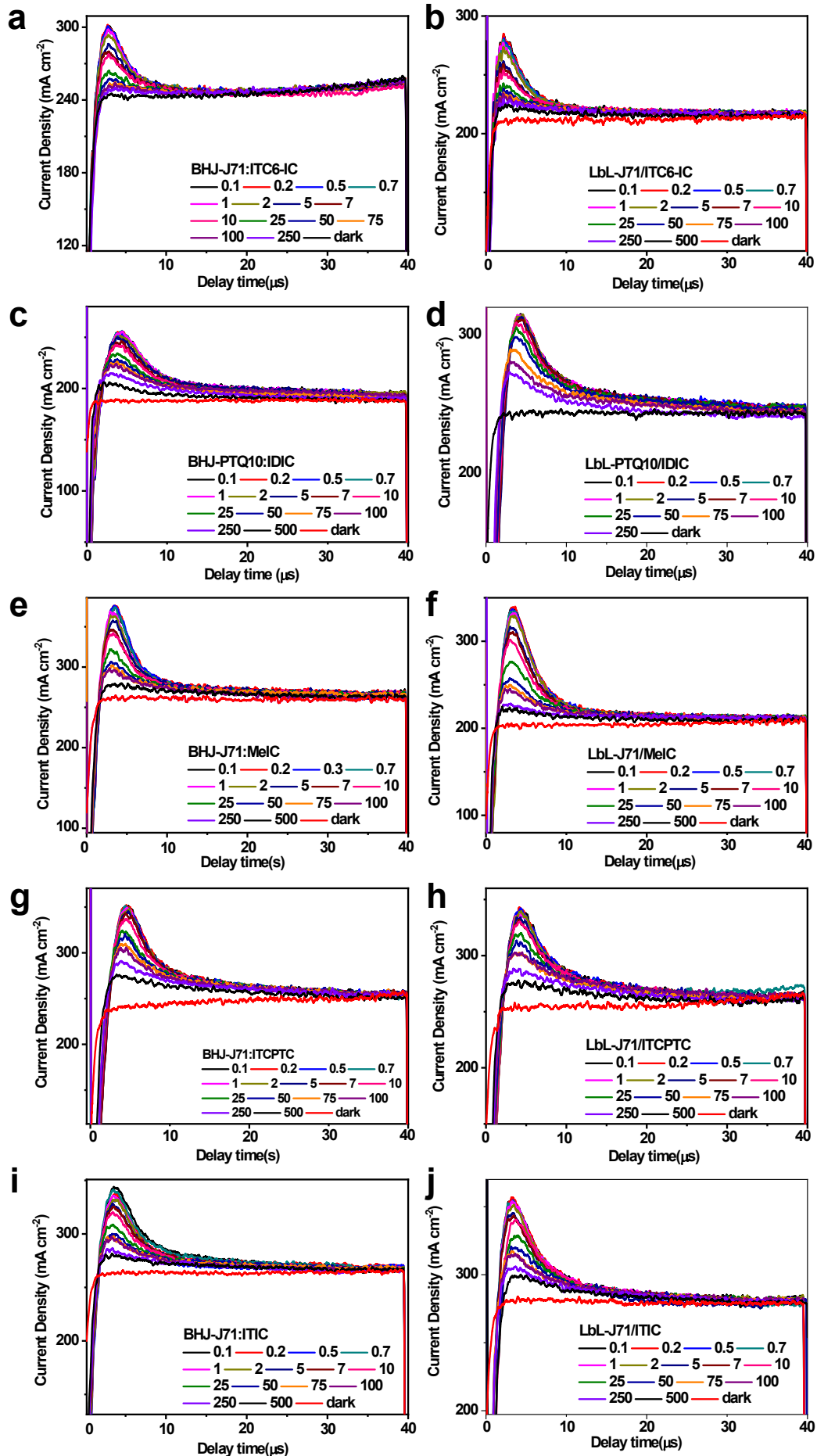


Figure S27. The Photo-CELIV traces for (a) J71:ITC6-IC BHJ, (b) J71/ITC6-IC LbL, (c) PTQ10:IDIC BHJ, (d) PTQ10/IDIC LbL, (e) J71:MeIC BHJ, (f) J71/MeIC LbL, (g) J71:ITCPIC BHJ, (h) J71/ITCPIC LbL, (i) J71:ITIC BHJ and (j) J71/ITIC LbL based devices for different delay times between the light pulse and the extraction voltage ramp.

Table S18. Parameters extracted from Photo-CELIV signals within these five different systems based on BHJ and LbL structures.

Active layers	Structure	μ [cm ² V ⁻¹ s ⁻¹]	n_0 (cm ⁻³)	τ_{tr} [s]	β_L [cm ³ s ⁻¹]	l_d [nm]
J71:ITC6-IC	BHJ	8.70×10^{-5}	5.55×10^{15}	2.30×10^{-7}	5.83×10^{-11}	379
	LbL	1.53×10^{-4}	3.15×10^{15}	1.31×10^{-7}	1.02×10^{-10}	466
PTQ10:IDIC	BHJ	6.80×10^{-5}	2.62×10^{15}	2.94×10^{-7}	4.55×10^{-11}	340
	LbL	7.81×10^{-5}	2.68×10^{15}	2.56×10^{-7}	5.23×10^{-11}	368
J71:MeIC	BHJ	3.79×10^{-5}	3.55×10^{15}	5.28×10^{-7}	2.54×10^{-11}	285
	LbL	4.43×10^{-5}	3.02×10^{15}	4.52×10^{-7}	2.96×10^{-11}	297
J71:ITCPIC	BHJ	6.07×10^{-5}	2.54×10^{15}	3.29×10^{-7}	4.06×10^{-11}	337
	LbL	6.18×10^{-5}	2.83×10^{15}	3.24×10^{-7}	4.14×10^{-11}	340
J71:ITIC	BHJ	4.93×10^{-5}	3.48×10^{15}	4.06×10^{-7}	3.30×10^{-11}	309
	LbL	5.07×10^{-5}	3.30×10^{15}	3.94×10^{-7}	3.40×10^{-11}	313

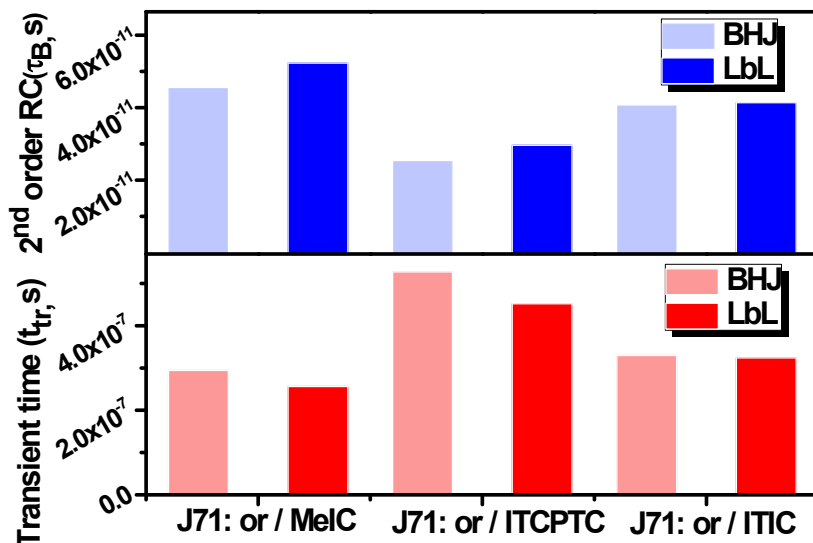


Figure S28. Second order recombination coefficient and transient time calculated from photo-CELIV measurements of solar cells based on J71 as donor and MeIC, ITCPIC and ITIC as acceptors.

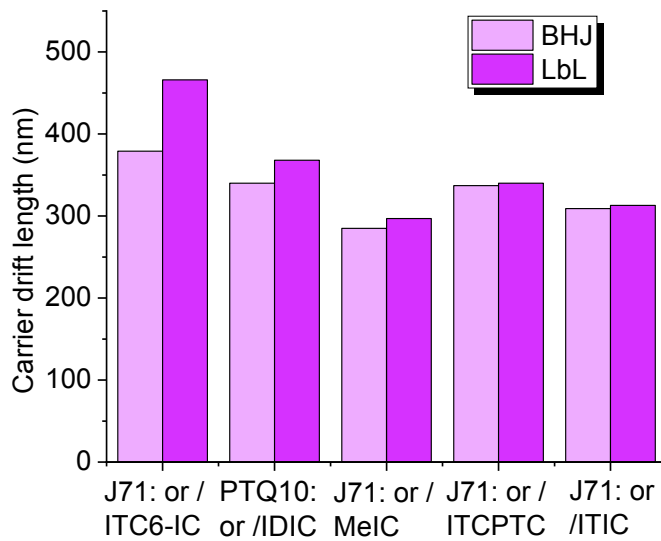


Figure S29. Carrier drift length extracted from photo-CELIV signals within these five different systems based on BHJ and LbL structures. Here the carrier drift length can be determined and calculated by the equation of $l_d^3 = \mu^2 U^2 e / J_{sc} \beta$.^[1] Where of μ is the mobility value of solar cell, U is assumed as the V_{oc} and β is Langevin recombination coefficient given by $\beta_L = e \times \mu / \varepsilon \times \varepsilon_0$.^[1, 2]

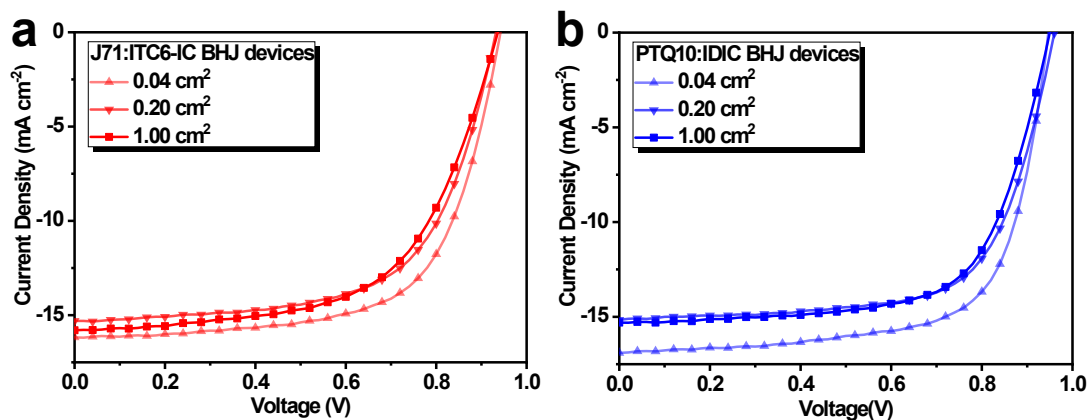


Figure S30. $J-V$ curves of the blade-coated BHJ OSCs with various device area based on (a) J71/ ITC6-IC, and (b) PTQ10/IDIC under the illumination of AM 1.5 G at 100 mW cm^{-2} .

Table S19. Photovoltaic parameters of the blade-coated BHJ devices with various device areas under the illumination of AM 1.5 G at 100 mW cm^{-2} .

active layer	Area [cm ²]	V_{oc} [V]	J_{sc} [mA cm ⁻²]	FF [%]	PCE (PCE ^a) [%]
J71/ITC6-IC	0.04	0.949	16.18	65.79	10.11 (10.04)

	0.20	0.952	15.35	63.66	9.14 (8.84)
	1.00	0.963	15.84	60.35	9.20 (8.96)
	0.04	0.947	16.91	68.97	11.04 (10.98)
PTQ10/IDIC	0.20	0.960	15.16	67.47	9.82 (9.52)
	1.00	0.949	15.30	66.63	9.04 (8.75)

^aThe values in square bracket are the average PCE obtained from 6 devices.

References

1. T. M. Clarke, D. B. Rodovsky, A. A. Herzing, J. Peet, G. Dennler, D. DeLongchamp, C. Lungenschmied and A. J. Mozer, *Adv Energy Mater*, 2011, **1**, 1062-1067.
2. J. Min, Y. N. Luponosov, N. Gasparini, M. Richter, A. V. Bakirov, M. A. Shcherbina, S. N. Chvalun, L. Grodd, S. Grigorian, T. Ameri, S. A. Ponomarenko and C. J. Brabec, *Adv Energy Mater*, 2015, **5**, 1500386.